Acta Crystallographica Section B
Structural Science
ISSN 0108-7681

Determination of zinc incorporation in the Zn-substituted gallophosphate ZnULM-5 by multiple wavelength anomalous dispersion techniques

M. Helliwell,[a]* J. R. Helliwell,[a] V. Kaucic,[b] N. Zabukovec Logar,[b] S. J. Teat,[c]‡ J. E. Warren[c]§ and E. J. Dodson[d]

[a]School of Chemistry, University of Manchester, Manchester M13 9PL, England, [b]National Institute of Chemistry, Hajdrihova 19, 1000 Ljubljana, Slovenia, [c]STFC, Daresbury Laboratory, Daresbury, Cheshire WA4 4AD, England, and [d]Department of Chemistry, University of York, Heslington, York YO1 5DD, England

‡ Current address: Advanced Light Source, Lawrence Berkeley National Laboratory, 1 Cyclotron Road, Berkeley, CA 94721, USA.
§ Current address: Department of Chemistry, University of Liverpool, Crown Street, Liverpool L69 7ZD, England.

Correspondence e-mail: madeleine.helliwell@manchester.ac.uk

Received 2 December 2009
Accepted 24 March 2010

The location of isomorphously substituted zinc over eight crystallographically different gallium sites has been determined in a single-crystal study of the gallophosphate ZnULM-5, $Ga_{(16-x)}Zn_x(PO_4)_{14}(HPO_4)_2(OH)_2F_7$, $[H_3N\{CH_2\}_6NH_3]_4$, $6H_2O$, in an 11 wavelength experiment, using data from Station 9.8, SRS Daresbury. The measurement of datasets around the K edges of both Ga and Zn, as well as two reference datasets away from each absorption edge, was utilized to selectively exploit dispersive differences of each metal atom type in turn, which allowed the major sites of Zn incorporation to be identified as the metal 1 and 3 sites, *M*1 and *M*3. The preferential substitution of Zn at these sites probably arises because they are located in double four-ring (D4R) building units which can relax to accommodate the incorporation of hetero atoms. As the crystal is non-centrosymmetric, with space group $P2_12_12$, it was also possible to use anomalous differences to corroborate the results obtained from the dispersive differences. These results were obtained firstly from difference Fourier maps, calculated using a phase set from the refined structure from data measured at the Zr *K* edge. Also, refined dispersive and anomalous occupancies, on an absolute scale, could be obtained using the program *MLPHARE*, allowing estimates for the Zn incorporation of approximately 22 and 18 at. % at the *M*1 and *M*3 sites to be obtained. In addition, f' and f'' values for Ga and Zn at each wavelength could be estimated both from *MLPHARE* results, and by refinement in *JANA*2006. The fully quantitative determinations of the dispersive and anomalous coefficients for Ga and Zn at each wavelength, as well as metal atom occupancies over the eight metal atom sites made use of the CCP4's *MLPHARE* program as well as *SHELXL* and *JANA*2006. The results by these methods agree closely, and *JANA*2006 allowed the ready determination of standard uncertainties on the occupancy parameters, which were for *M*1 and *M*3, 20.6 (3) and 17.2 (3) at %, respectively.

1. Introduction

Microporous phosphate-based molecular sieves have many applications as solid acid catalysts (Hartmann & Kevan, 1999). Their properties are often modified by the incorporation of hetero metal atoms, which are isomorphously substituted into the framework of the material. To understand the properties of these materials requires the determination of the framework structure, the location of non-framework species, such as template structure-determining species, as well as finding the site(s) of the substituted metal atoms. The latter is often the most difficult to determine, since the substituted metal atom is often close in atomic number to the dominant metal atom species and is normally present at low occupancy as well as

being at the same site(s) as the metal at higher concentration. Thus, although the geometry of the framework and position of the template atoms can be determined by single wavelength techniques, it is not usually possible to locate the substituted metal atom positions owing to the similarity of the atomic scattering factors. One method of addressing this problem is to use the multiple-wavelength anomalous dispersion (MAD) technique. This exploits the large changes in the atomic scattering factor which take place close to the absorption edges of elements, due to the variation of f' and f'' with wavelength. The atomic scattering factor is given by

$$f = f^0 + f' + if'', \quad (1)$$

where f^0 is the scattering factor of the unperturbed atom, and f' and f'' are the real and imaginary components of the anomalous scattering. The signals arising from the real and imaginary parts will be referred to below as dispersive and anomalous. By tuning to the absorption edge of a specific element in a sample to stimulate large changes in f' with wavelength, it is possible to induce such dispersive differences in those reflection intensities which have a large contribution from the metal atom sites in question. After appropriate scaling of the data measured at different wavelengths and calculation of a suitable phase set, it is then possible to determine the site(s) of the metal atom either by calculation of a difference Fourier map, or by refinement of the occupancies. We have used such techniques to determine the site of Co incorporation in the zincophosphate CoZnPO-CZP in a multiple (five) wavelength experiment (Helliwell *et al.*, 1999). More recently, Cowley *et al.* (2002) distinguished isoelectronic zinc and gallium cations in the framework of three zinc-gallium phosphates using MAD methods and data measured at SRS Daresbury Laboratory, Station 9.8. For non-centrosymmetric samples, it is also possible to exploit the large changes in f'' close to the absorption edge, which lead to the non-equivalence of Friedel pairs of reflections and can allow the calculation of what are termed anomalous difference maps, to determine the metal atom positions. Several reviews of the use of anomalous scattering in structural chemistry and biology are available (Cheetham & Wilkinson, 1992; Hodeau *et al.*, 2001; Cianci *et al.*, 2005). In addition to neighbouring atom contrast applications, anomalous scattering can also be used for valence contrast experiments (see above reviews, and for example Wu *et al.*, 1998) and for the determination of absolute structure (Flack & Bernardinelli, 1999).

The subject of this study is the determination of the sites of Zn incorporation in the gallophosphate, ZnULM-5, which has the formula $Ga_{(16-x)}Zn_x(PO_4)_{14}(HPO_4)_2(OH)_2F_7$, $[H_3N\{CH_2\}_6NH_3]_4$, $6H_2O$, and crystallizes in the space group $P2_12_12$; EDAX (Energy Dispersive Analysis by X-ray) analysis results of a representative group of five crystals show that the zinc is substituting gallium in the framework by 3–6% by weight. The structure of the pure gallium ULM-5 was determined by Loisseu & Ferey (1994). That of ZnULM-5 was determined originally using Cu $K\alpha$ radiation (Mrak *et al.*, 2001) and this showed that incorporation of Zn leads to expansion of the unit cell owing to the larger ionic radius of Zn^{2+} *versus* Ga^{3+} ($Ga^{3+}-O \simeq 1.82$ Å, $Zn^{2+}-O \simeq 1.95$ Å). The framework structure contains 16-, eight- and six-membered rings and four-, five- and six-coordinate metal atom sites and the 16-membered ring has dimensions of 12.2 × 8.34 Å. Owing to the lack of scattering contrast between Zn and Ga with Cu $K\alpha$ radiation, the site(s) of Zn substitution could not be determined directly by refinement of the relative occupancies. However, a careful examination of bond lengths suggested that there may be incorporation of Zn on the five- and six-coordinate framework sites, but the bond lengthening was only significant at the trigonal pyramidal Ga3 site, which suggested a higher incorporation at this position.

Thus, X-ray resonant scattering to stimulate maximal changes in the anomalous dispersion was required to determine the site(s) of incorporation of Zn, where the Zn *K* edge is at 1.285 Å, and that of Ga is at 1.195 Å. Although this study is similar to that of Cowley *et al.* (2002) in that isoelectronic Zn^{2+} substitution was to be determined at the eight Ga^{3+} sites, the experiment was much more challenging because the proportion of Zn is much lower (3–6 wt % in ZnULM-5 *versus* between 9 and 15 wt % for the three compounds in Cowley *et al.* (2002). Moreover, because the sample is non-centrosymmetric, the possibility of exploiting the anomalous signal was viable. Therefore, in order to obtain accurate estimates of the Zn incorporation over the eight metal atom sites, utilizing both the dispersive and anomalous signals, it was necessary to collect multiple wavelength datasets around the Zn and Ga *K* edges, in order to selectively vary the dispersive signal of each metal in turn as well as choosing additional wavelengths to maximize the anomalous signals (Helliwell *et al.*, 2005). Synchrotron radiation data collection was carried out at Station 9.8 Daresbury (Cernik *et al.*, 1997) at multiple wavelengths around both the Zn and Ga *K* edges, as well as at remote wavelengths, and the results of the analyses of these data are the subject of this paper. In particular, since the analysis procedures for analyzing resonant scattering data to determine dopant site(s) from single crystals is not well documented, a thorough exploration and comparison of available methodology is given, including the use of the CCP4 program suite (Collaborative Computational Project, Number 4, 1994), *SHELXL* (Sheldrick, 2008) and *JANA*2006 (Petricek *et al.*, 2006).

2. Methods

2.1. Experimental

The Si(111) monochromator used on SRS 9.8 was a triangular focusing design. This type of monochromator and its spectral bandwidth properties have been extensively characterized by Helliwell *et al.* (1982; summarized in Helliwell, 1984). With the curvature of such a monochromator carefully set and the horizontal acceptance slits restricted, as well as a fine focus at the sample, it is possible to obtain a reasonably fine spectral bandpass of approximately 1×10^{-4}, *i.e* approximately 1 eV. Thus, even white-line absorption-edge details can be resolved in detail; see Arndt *et al.* (1982) for a

Table 1
Summary of the 11 synchrotron datasets measured at different wavelengths; the f' and f'' values are from Sasaki (1989) for pure Zn and Ga metal (oxidation state 0).

See Fig. 1 for these wavelength settings with respect to each metal *K* edge.

Dataset	Wavelength (Å)	Energy (KeV)	Zn f', f'' (e)	Ga f', f'' (e)
1 = Zn f''_{max}	1.2739	9.7327	−4.88, 3.88	−2.53, 0.55
2 = about to drop off Zn f''_{max}	1.2771	9.7083	−5.66, 3.89	−2.42, 0.56
3 = Zn f'_{min}	1.2803	9.6840	−11.52, ∼2	−2.42, 0.56
4 = base of Zn edge	1.2846	9.6516	−5.39, 0.49	−2.42, 0.56
5 = further along base of Zn edge	1.2889	9.6194	−4.67, 0.49	−2.33, 0.56
6 = still further along base of Zn edge	1.2996	9.5402	−4.02, 0.50	−2.25, 0.57
7 = between Zn and Ga edges	1.2320	10.064	−2.39, 3.58	−3.22, 0.52
8 = Ga f'_{min}	1.1923	10.399	−1.76, 3.39	−7.67, 3.89
9 = Ga f'_{min}	1.1928	10.394	−1.76, 3.39	−10.42, ∼2
10 = Ga f''_{max}	1.1848	10.465	−1.63, 3.35	−4.53, 3.84
11 = Zr edge reference wavelength	0.6787	18.268	0.22, 1.33	0.17, 1.50

rhenium complex single-crystal LIII absorption edge f' study on SRS 7.2. Previous experience on 9.8 has also shown that over the time scale of these experiments the wavelength is stable to less than 1 eV. In the absence of a fluorescence detector the *K* absorption edge positions of Ga and Zn in ZnULM-5 were determined by measurement of transmission curves for zinc and gallium oxides, compounds that are expected to have similar K absorption edges and positions as the Zn and Ga atoms in ZnULM-5 due to the oxidation states being the same. Since the Ga concentration is much greater than that of Zn, the signal from Ga was expected to be significant at the Zn *K* edge, and therefore a total of six crystallographic datasets were collected around the Zn edge position to allow optimal subtractions between datasets to be made; these datasets were measured at the f' minimum, the f'' maximum as well as three at the base of the Zn absorption edge. Further datasets were measured at the f' dip and f'' maximum for Ga, and also between the Zn and Ga absorption edges, and a final reference dataset was collected at the Zr *K* absorption edge, making a total of 11 datasets, which are summarized in Table 1 (with expected values given of f' and f'' from Sasaki, 1989); see also Fig. 1. Each dataset was measured to an excellent diffraction resolution of at least 0.85 Å, and high data completeness. The data were then processed using *SAINT* (Bruker, 2002), and *SADABS* absorption corrections were applied (Bruker, 2001*b*).

All 11 datasets were converted into a form suitable for input into the CCP4 Program Suite (Collaborative Computational Project, Number 4, 1994), with Friedel pairs separate, using *SCALEPACK* (Otwinowski & Minor, 1997). Then the programs *SCALEPACK2MTZ* and *TRUNCATE* were used to convert intensities into structure factor amplitudes, in the mtz format, with the anomalous differences calculated. The program *CAD* was used to combine the datasets into the same file. A phase set for X-ray dispersive and anomalous difference Fourier electron density maps was calculated using *SHELXL*97 (Sheldrick, 2008), by anisotropic refinement of the atomic model against the reference Zr *K* edge dataset 11, and assuming that the metal atom sites were fully occupied by gallium. It was not possible to obtain sufficiently accurate phases whilst leaving out the Ga metal atom sites completely, *i.e.* to arrive at a 'protein crystallographer style' omit map approach. Data scaling was carried out using the CCP4 program *SCALEIT*, and after a number of trials of scaling with use of:

(i) an overall scale factor,
(ii) isotropic and
(iii) anisotropic scaling,

it was found that optimum results in terms of peak-to-background in the difference maps were achieved using an overall scale factor to place all the datasets onto the same scale. Data scaling to F_o from the final refinement of the structure using dataset 11 allowed all the datasets to be placed on an approximately absolute scale. The CCP4 program *FFT* was then used to calculate dispersive difference Fourier maps ($\Delta f'$) and anomalous difference maps.

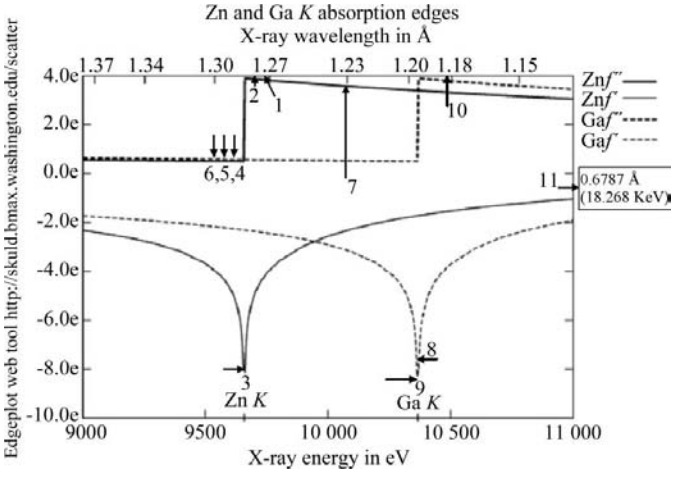

Figure 1
Absorption edges of Zn and Ga, with approximate wavelength positions of the 11 datasets collected at Station 9.8 Daresbury shown as labels.

2.2. Refinement of the basic model using the reference dataset

Refinement of the structure using *SHELXL* (Sheldrick, 2008) within the *SHELXTL* package (Bruker, 2001*c*) was carried out against dataset 11, with parameters from the Cu *K*α model refinement used as a starting point (Mrak *et al.*, 2001). The crystal data are summarized in Table 2[1] and a plot of the unique portion of the framework of the structure is shown in Fig. 2(*a*). The eight metal atom positions of the asymmetric unit viewed down **a** are shown in Fig. 2(*b*). As in the Cu *K*α refinement and that of the Zn-free analogue (Mrak

[1] Supplementary data for this paper are available from the IUCr electronic archives (Reference: HW5009). Services for accessing these data are described at the back of the journal.

et al., 2001; Loiseau & Ferey, 1994), it was found that the *M*2 site consistently showed a higher U_{eq} value than the other seven metal atom sites, suggesting possible disorder, or that the site was partially vacant. In fact, by dividing this site into two disordered components with occupancies summing to 1.0, and anisotropic refinement, it was shown that the disordered components, which are separated by 0.59 (2) Å, now had similar U_{eq} values to the other metal atom sites, and moreover, the conventional *R* value was considerably reduced from to 0.045 to 0.037, indicating that the *M*2 site is slightly disordered.

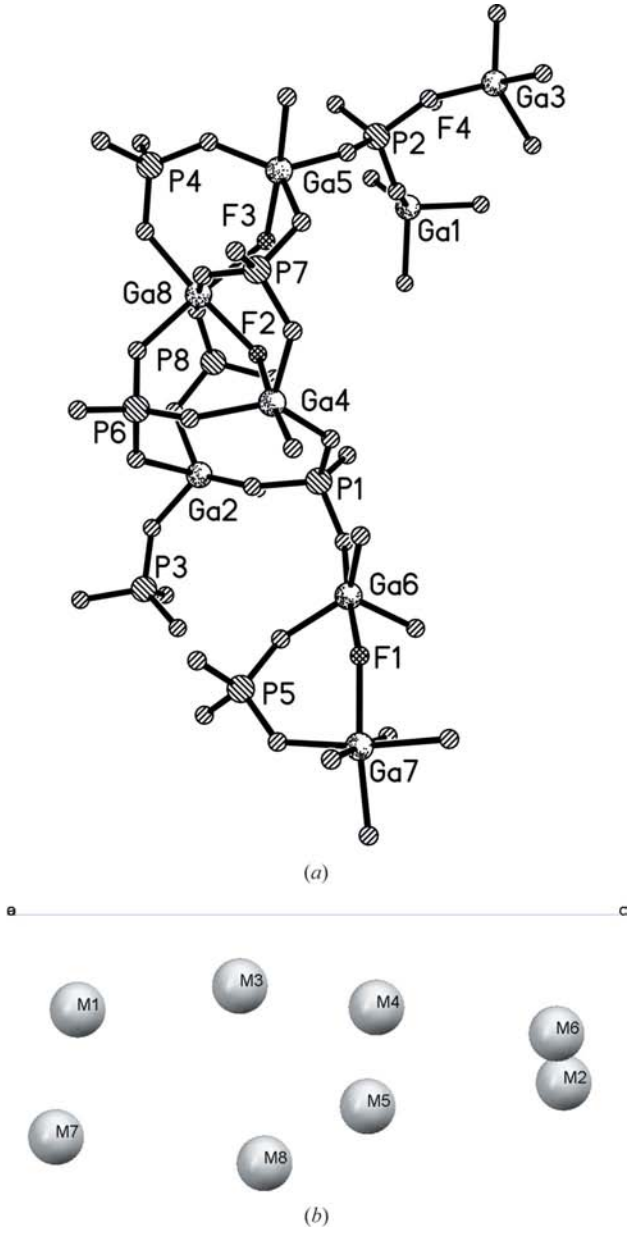

Figure 2
(*a*) Plot of a portion of the framework of ZnULM-5 showing the four-, five- and six-coordinate metal atom sites. All the P atoms are tetrahedral. (*b*) Plot of the eight metal atom positions in the asymmetric unit viewed down **a** (and the same view is adopted in Figs. 3–6).

Table 2
Crystal data for ZnULM-5 with refinement using dataset 11.

Crystal data	
Chemical formula	$Ga_{(16-x)}Zn_x(PO_4)_{14}(HPO_4)_2(OH)_2F_7$, $[H_3N\{CH_2\}_6NH_3]_4$, $6H_2O$
M_r	3374.35
Crystal system, space group	Orthorhombic, $P2_12_12$
Temperature (K)	293
a, *b*, *c* (Å)	24.814 (13), 18.458 (5), 10.2575 (18)
V (Å^3)	4698 (3)
Radiation type	Synchrotron, λ = 0.67870 Å
μ (mm^{-1})	4.85
Crystal size (mm)	0.45 × 0.07 × 0.05
Data collection	
Diffractometer	CCD area detector
Absorption correction	Multi-scan *SADABS*
T_{min}, T_{max}	0.715, 1.000
No. of measured, independent and observed [$I > 2\sigma(I)$] reflections	32 739, 7609, 7569
R_{int}	0.026
Completeness to θ = 23.83° (%)	91.8
Refinement	
$R[F^2 > 2\sigma(F^2)]$, $wR(F^2)$, *S*	0.037, 0.094, 1.07
No. of reflections	7609
No. of parameters	668
No. of restraints	213
H-atom treatment	H-atom parameters constrained
$\Delta\rho_{max}$, $\Delta\rho_{min}$ (e Å^{-3})	1.01, −0.72

Computer programs used: *SMART* (Bruker, 2001*a*), *SAINT* (Bruker, 2002), *SHELXS*97, *SHELXL*97 (Sheldrick, 2008), *SHELXTL* (Bruker, 2001*c*).

2.3. Computational modelling of the metal atom occupancies

2.3.1. *MLPHARE*. *MLPHARE* is a CCP4 program for phase determination in biological macromolecules using dispersive and anomalous scattering differences, including MAD data sequences. *MLPHARE*, as a standard step, allows the refinement of dispersive and anomalous occupancies for each metal atom site for each wavelength. The dispersive occupancies for each metal atom site arise from the differences in f' between datasets measured at two different wavelengths and the anomalous occupancies at each metal atom site arise from the f'' value at a particular wavelength. A coordinates file with the final positions of the metal atoms from the refinement against dataset 11, and U_{iso} values calculated from the refined U_{eq} values was used (see supplementary Table S8). The disordered *M*2 site was treated as a single fully occupied site, but with a larger U_{iso} value than for the other metal atoms. Real and anomalous occupancies were calculated using the various datasets as the 'native' and datasets measured at different wavelengths chosen as 'derivatives'. Since the datasets have been scaled to be on an approximately absolute scale, the occupancies in electrons should represent the values of $\Delta f'$ and f'' for each metal atom at each metal atom site.

In order to eliminate the signal due to differences in f' for Zn, the native could be chosen as dataset 10, and the derivatives as datasets 8 and 9, columns D10-8 and D10-9 (Table S6*a*). Refined values of the f'' values for datasets 8, 9 and 10 are also shown (ANO 8, 9 and 10) as well as $\Delta f'$ values with these three datasets as derivatives and datasets 7 and 11 as natives. Table S6(*b*) shows the values of f'' for datasets 1, 2 and 3 (ANO1, 2 and 3) and the $\Delta f'$ values between dataset 3

as the derivative and datasets 4, 5, 6, 7 and 11 as the native, thus allowing the signal owing to the Zn incorporation to be derived. The MLPHARE calculation involving probability estimates of reflection phases from Harker phase diagrams, also yields 'best-phase' estimates (Blow & Crick, 1959). These best phases were checked to see that the whole framework structure was thereby determined from the MAD signals for the Ga and Zn. Thus, the mean figure of merit for the phases using all datasets against dataset 7 was 0.96 corresponding to a mean phase error of 16°. The display of the peaks derived from this electron density map is shown in supplementary Fig. S1 and a close-in view of a phosphate in Fig. S2. The structure generated using phases from *MLPHARE* was checked by refinement with *SHELXL*, which showed that all the framework atoms had been determined, and that there was only one erroneous atom site. To obtain phases of this very high quality to a diffraction resolution of 0.85 Å is a useful benchmark of the effectiveness of *MLPHARE* and is perhaps a record for MAD phases determination quality!

2.3.2. Refinement of occupancies using *SHELXL*. The method adopted by Cowley *et al.* (2002) for refinement of the occupancies of each metal atom site was tried as follows: using the final refined model from the Zr data, the occupancies of each metal atom site were refined to convergence as mixed Zn/Ga, with occupancies constrained to sum to 1.0, using the absorption edge data. The initial occupancies were set to 50:50 for each metal atom site. Then refinement of the structure, but not the metal occupancies, was carried out with the Zr-edge dataset 11, using occupancies fixed at the values obtained from the refinement with the absorption edge data. The Zn f' dip dataset 3, and the Ga f' dip datasets 8 and 9 were tested. The values of f' and f'' for Zn for dataset 3 were set at those obtained from the *MLPHARE* results, whilst those from Sasaki (1989, Table 1) were used for Ga. Likewise, *MLPHARE* values of f' and f'' for Ga were employed for refinement against datasets 8 and 9, with the Sasaki values shown in Table 1 used for the Zn parameters. No restraint was placed on the overall Zn composition. The disordered metal atom site *M*2 was not included in the refinement of the Ga/Zn occupancies, but defined as a Ga atom disordered over two sites. In this way, alternate refinement with the absorption edge data, followed by the dataset 11 was carried out until convergence was reached, which took about two rounds of this cycle.

Finally, to test the sensitivity of the method to the possible errors in the values f' and f'' close to the Zn or Ga absorption edges, these rounds of refinement were repeated with values of f' and f'' changed by up to ± 1 electron, as suggested by Zhang *et al.* (2003).

2.3.3. Multi-wavelength refinement using *JANA*2006. Multi-wavelength refinement of site occupancies with powder diffraction data has been shown to yield precise results (Zhang *et al.*, 2003, 2005), although there is the difficulty of defining suitable values for f' and f'' for each wavelength. In Zhang *et al.* (2005), values of f' and f'' for wavelengths measured close to the absorption edges were determined from fluorescence scans, and for wavelengths remote from the absorption edges, values from *FPRIME* (Cromer, 1983) were employed. Although we were not able to estimate the anomalous dispersion coefficients directly from fluorescence scans, refinement of dispersive and anomalous occupancies using *MLPHARE*, as described above, has allowed the determination of reasonable values of f' and f'' for wavelengths 3, 8, 9 and 10, *i.e.* those that are very close to the absorption edges of Zn or Ga. Alternatively, since *JANA*2006 allows the determination of refined values of f' and f'' at each wavelength, then these values can be used for a multi-wavelength refinement of the occupancies. For wavelengths relatively remote from the absorption edges, values shown in Table 1 taken from Sasaki (1989), could be employed. However, since *JANA*2006 automatically generates values of f' and f'' for general wavelengths, including synchrotron data, then for the datasets which are reasonably far from the absorption edges, *JANA* values, which are similar to those in Table 1, could be employed.

In order to compute suitable dispersive and anomalous coefficients using *JANA*2006, the final refined structure from *SHELXL* using the reference wavelength 11 was imported into *JANA*2006, and the framework was refined anisotropically in *JANA* against wavelength 11 until convergence was reached. Then each wavelength in turn was imported into *JANA*, and refinement of the scale factor, and f' and f'' values was carried out. Two different occupancy models were used, the first with the gallium occupancies of *M*1 and *M*3 fixed at the values derived from *MLPHARE* (0.78 and 0.82) and with the occupancies of *M*4 to *M*8 set at 1.0 (Model 1). In the second case, since the *SHELXL* refinement of the occupancies using the anomalous datasets suggested a small percentage of Zn at each of the sites *M*4 to *M*8, the occupancies of these atoms were set at Ga4–Ga8 = 0.95, Zn4–Zn8 = 0.05 (with Ga occupancies of 0.78 and 0.82 for *M*1 and *M*3) (Model 2). In each of Models 1 and 2, the disordered *M*2 site was assumed to be gallium only.

The multi-wavelength refinement was then carried out using 10 wavelengths (the maximum allowed by *JANA*2006), omitting dataset 5 (one of the three datasets measured at the base of the Zn K edge). Again, refinement of the framework atoms was carried out to convergence against wavelength 11. Then the reflection files 1–4 and 6–10 were imported into *JANA*2006, with f' and f'' values for each wavelength measured close to the absorption edge of Zn or Ga set firstly to the values from *MLPHARE*, secondly to the values from *JANA* using Model 1, and thirdly with values derived using the occupancy Model 2. Values of f' and f'' for wavelengths more remote from either the Zn or Ga absorption edges were input either from Table 1, or not altered from those input by *JANA*2006 for that wavelength, which are similar to those in Table 1 from Sasaki (1989); the values of the dispersive and anomalous coefficients used for each refinement are shown in Table S7. In a final refinement, Ga and Zn values of f' and f'' for each wavelength from Table 1 (Sasaki, 1989) were employed.

For the multi-wavelength refinements, in each case, approximate scale factors for each wavelength were included

Table 3
Dispersive difference map summary showing peak heights in electrons, peak heights/r.m.s. (metal atom assignment), calculated with coefficients $|F_{ref} - F_{Znf'}|$, where $F_{Znf'}$ is dataset 3 and F_{ref} are the reference datasets 11 and 5.

See also Table S1 for the full results. The values of $Zn\Delta f'$ and $Ga\Delta f'$ are estimated from Sasaki (1989) (Table 1).

λ_{11}–λ_3 ($Zn\Delta f' = 11.3$, $Ga\Delta f' = 2.2$ e)	λ_5–λ_3 ($Zn\Delta f' = 6.8$, $Ga\Delta f' = 0$ e)
4.41, 17.9 (*M*1)	1.16, 18.6 (*M*1)
4.29, 17.4 (*M*3)	0.98, 15.7 (*M*3)
3.63, 14.8 (*M*4)	0.25, 4.0
3.48, 14.1 (*M*7)	0.25, 4.0
3.44, 14.0 (*M*6)	
3.08, 12.5 (*M*8)	
2.69, 10.9 (*M*5)	
1.95, 7.9 (*M*2)	
1.11, 4.5	

from the single wavelength refinements used to obtain the f' and f'' values. In the first round of refinement, the scale factors for each wavelength were refined. Metal atom occupancies were then refined, with the sum of the Ga and Zn components constrained to sum to unity (excluding the disordered atom, site *M*2). This was followed by refinement of the metal occupancies, coordinates and anisotropic displacement parameters. Finally, the other framework atoms were refined anisotropically to convergence. It was also possible to use reduced numbers of wavelengths, to check the effect on the refined occupancies. If only one wavelength was used (either wavelength 3 or 9, closest to the f' dip for Zn and Ga), then only the occupancies of the metal atoms were refined, with other parameters being fixed.

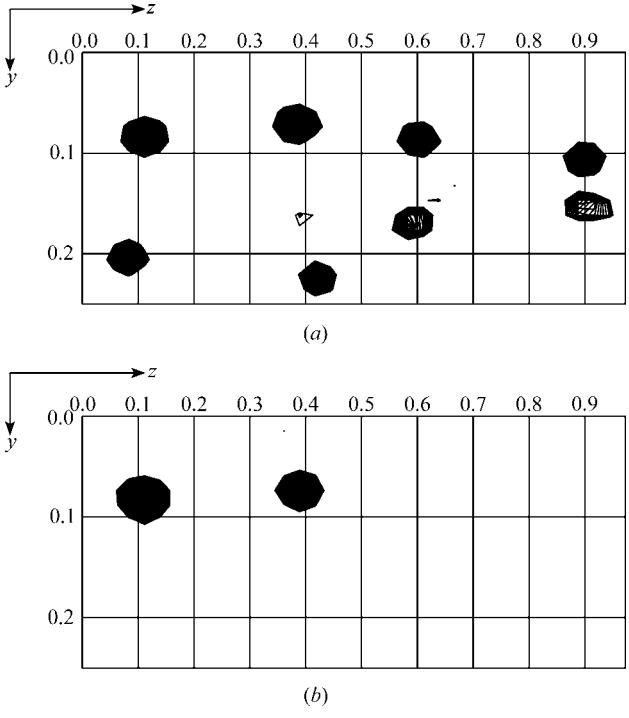

Figure 3
Dispersive difference Fourier maps calculated with the Zn f' dip dataset 3, using coefficients (*a*) $|F_{11} - F_{Znf'}|$, (*b*) $|F_5 - F_{Znf'}|$.

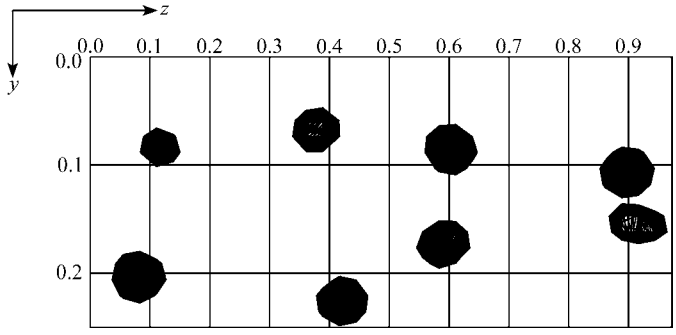

Figure 4
Dispersive difference Fourier map calculated with the Ga f' dip dataset 9, using coefficients $|F_7 - F_{Gaf'}|$.

3. Results

3.1. Calculation of dispersive difference Fourier electron-density maps

3.1.1. Zn *f′* dip. Dispersive difference maps were calculated using the coefficients $|F_{ref} - F_{Znf'}|$, where $F_{Znf'}$ is dataset 3 (Table 1) and F_{ref} is one of several possible reference wavelengths each yielding a difference in Zn f' value with respect to wavelength 3. Fig. 3(*a*) shows the dispersive difference map with F_{ref} = dataset 11, the Zr *K* edge data. This shows peaks at each of the metal atom sites, but the peak heights corresponding to the *M*1 and *M*3 sites are significantly larger than those at the other metal atom sites (Table 3), suggesting that incorporation of Zn has taken place to a greater extent at these sites. Since there is a significant difference in f' for Ga of over 2 electrons between these two wavelengths (Table 1), part of the observed signals in the dispersive difference maps could be due to this. In order to cancel out the signal due to Ga, one of the datasets measured close to the Zn *K* edge (1, 2, 4, 5, 6, 7) could be chosen as the reference wavelength, whilst still giving a significant f' difference for Zn (Table 1). Difference Fourier maps calculated with these datasets chosen as references each show only two significant peaks above the background, namely at the *M*1 and *M*3 sites (see Table 3 and Fig. 3*b*) for example; Table S1 shows the complete results calculated with all the possible reference datasets), thus confirming that the Ga signal has been subtracted out, and indicating that Zn substitution has taken place at these sites only, with a slightly greater incorporation at the *M*1 site. There were some peaks between 3 and 4 r.m.s.[2] which are obviously not chemically meaningful and provide an estimate of the noise floor of the calculations and the MAD data.

3.1.2. Ga *f′* dip. Two datasets, 8 and 9, were measured on the rise of the Ga *K* edge, and it was only after data scaling that it became clear that the largest dispersive difference for Ga occurred for dataset 9 (see Table S5), so this dataset was

[2] r.m.s. refers to the root mean square of the difference electron density in the unit cell.

Table 4
Dispersive difference-map summary showing peak heights in electrons, peak heights/r.m.s. (metal atom assignment), calculated with coefficients $|F_{\rm ref} - F_{{\rm Ga}f'}|$, where $F_{{\rm Ga}f'}$ is dataset 9 and $F_{\rm ref}$ is the reference dataset number 7; see also Table S2 for the full results.

The values of Zn$\Delta f'$ and Ga$\Delta f'$ are estimated from Sasaki (1989) (Table 1).

λ_7–λ_9 (Zn$\Delta f'$ = 0.6, Ga$\Delta f'$ = 7.2 e)
10.22, 21.2 (*M*7)
9.97, 20.7 (*M*6)
9.91, 20.6 (*M*4)
9.40, 19.5 (*M*8)
8.10, 16.8 (*M*5)
6.83, 14.2 (*M*3)
5.42, 11.3 (*M*1)
4.97, 10.3 (*M*2)
1.62, 3.4

thereby determined to be at the Ga f' dip. Dispersive difference maps were calculated using the coefficients $|F_{\rm ref} - F_{{\rm Ga}f'}|$, where $F_{{\rm Ga}f'}$ is dataset 9, and the reference datasets are 7, 8, 10 and 11; the key results are shown in Table 4 (Table S2 shows the complete results using all the possible reference datasets). The choice of these reference datasets allows the Zn signal to be subtracted out, so that the peaks on the maps only show the Ga signal (Fig. 4). In each case, there are peaks at each of the metal atom sites, with the four highest all having similar peak heights Tables 4 and S2), suggesting that these sites are fully occupied by Ga; these are the *M*4, *M*6, *M*7 and *M*8 sites. The *M*5 site is consistently the fifth highest, followed by the *M*3 and *M*1 sites, and finally the *M*2 site. From the dispersive difference Fourier maps at the Zn *K* edge described above, the reduced peak heights at the *M*3 and *M*1 sites is expected, since it was shown that Zn incorporation had taken place at these two sites. The *M*5 peak height is only slightly lower than those of the fully occupied Ga sites, but the *M*2 site is consistently about half the height, suggesting that this site is partially vacant or has reduced order compared with the other metal atom sites. There is no indication of any Zn incorporation at the *M*5 and *M*2 sites (or at the *M*4, *M*6 *M*7 and *M*8 sites) from the dispersive difference maps calculated at the Zn *K* edge.

3.2. Anomalous difference maps

3.2.1. At the Zn *K* edge. Table 1 shows that there are significant f'' signals for Zn for datasets 1, 2, 3 and 7, whilst that for Ga is only ~ 0.5 electron in each case. Anomalous difference maps, calculated using each of these datasets, showed just two peaks above the background, at the *M*1 and *M*3 sites (Table 5, Fig. 5 for key results and Table S3 for the complete results), clearly demonstrating the significant Zn incorporation at these two sites, and corroborating the results obtained from the dispersive difference maps calculated using the Zn f' dip data. The peak heights are reduced for dataset 3 compared with the others, which is to be expected since this dataset was measured at a position half-way up the Zn *K* absorption edge, so that the f'' value is expected to be ~ 2 electrons, rather than ~ 3.5 electrons for the other three datasets. An anomalous difference map calculated with

Table 5
Peaks heights for anomalous difference maps, showing peak heights in electrons, peak heights/r.m.s. (metal atom assignment), calculated for dataset 1 and 3, where there is a significant anomalous difference for Zn (see also Table S3).

The values of Zn$f''$and Gaf'' are from Sasaki (1989) (Table 1).

λ_1 (Znf'' = 3.9, Gaf'' = 0.5 e)	λ_3 (Znf'' = 2, Gaf'' = 0.6 e)
1.72, 18.7 (*M*1)	1.30, 13.5 (*M*1)
1.18, 12.8 (*M*3)	1.08, 11.3 (*M*3)
0.38, 4.1	0.39, 4.1

dataset 6, where the f'' values for both Zn and Ga are expected to be very small (Table 1), shows no peaks at any of the metal atom sites.

3.2.2. At the Ga *K* edge. Dataset 10 was measured at the top of the *K* absorption edge for Ga, and corresponds to the f'' maximum for this metal. However, since the absorption edges of Zn and Ga are rather close in energy, there is also a significant f'' signal for Zn at this wavelength (Table 1). The anomalous difference map for dataset 10 shows peaks at all the metal atom sites (Table 6, and Fig. 6*a*). The top four are those at the *M*4, *M*6, *M*7 and *M*8 sites, which from the dispersive difference Fourier maps are assumed to be fully occupied by Ga. The *M*3 and *M*1 sites, determined to be the sites of significant Zn incorporation, are the fifth and eighth highest peaks. The *M*5 and *M*2 sites are seventh and tenth highest, and there are peaks that cannot be assigned, which are sixth and ninth highest. As expected from the similar values of f'' for Zn and Ga for dataset 8 to those of dataset 10, in the anomalous difference map calculated with dataset 8, peaks are obtained in a similar order, although the *M*2 site appears as the twentieth highest peak (Table S4). However, because dataset 9 is measured half-way up the Ga *K* absorption edge, and can therefore be expected to have a value for Ga f'' of about 2 electrons *versus* 3.4 electrons for Zn, the *M*1 and *M*3 peaks become enhanced, owing to the Zn substitution at these sites. These two peaks are followed by those arising from the fully occupied Ga sites, *M*4, *M*6, *M*7 and *M*8 (Table 6, Fig. 6*b*).

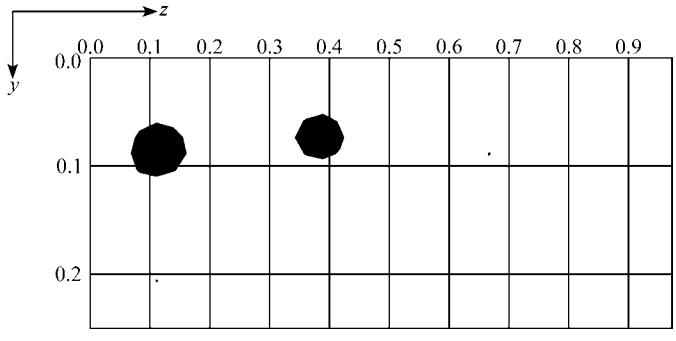

Figure 5
Anomalous difference Fourier map calculated with dataset 1, at the f' maximum for Zn.

Table 6
Peaks heights for anomalous difference maps, showing peak heights in electrons, peak heights/r.m.s. (metal atom assignment), calculated for datasets 9 and 10, where there is a significant anomalous difference for both Ga and Zn, which is reduced for Ga for dataset 9 (see also Table S4).

The values of Znf'' and Gaf'' are from Sasaki (1989) (Table 1). Those peaks marked (?) are at positions which cannot be related to one of the eight metal atom sites

λ_9 (Znf'' = 3.4, Gaf'' = 2 e)	λ_{10} (Znf'' = 3.3, Gaf'' = 3.8 e)
1.88, 9.4 (*M*1)	4.94, 9.8 (*M*7)
1.74, 8.7 (*M*3)	4.84, 9.7 (*M*4)
1.50, 7.5 (*M*6)	4.77, 9.5 (*M*6)
1.48, 7.4 (*M*4)	4.62, 9.2 (*M*8)
1.44, 7.2 (*M*7)	3.37, 6.8 (*M*3)
1.39, 7.0 (*M*8)	3.08, 6.2 (?)
1.09, 5.5 (?)	2.85, 5.7 (*M*5)
1.03, 5.2 (*M*5)	2.8, 5.7 (*M*1)
0.93, 4.6 (?)	2.45, 4.9 (?)
0.84, 4.2 (*M*2) peak 15	2.45, 4.9 (*M*2) Peak 10

3.3. Metal occupancy refinement results from *MLPHARE*, *SHELXL* and *JANA*2006 and f' and f'' values from *MLPHARE* and *JANA*2006

Three methods were employed for comparison to obtain refined metal atom occupancies, namely *MLPHARE*, *SHELXL* and *JANA*2006. In addition, it was also possible to derive values of f' and f'' using *MLPHARE* and *JANA*2006. The full dispersive and anomalous values for each metal atom site, on an approximately absolute scale, from *MLPHARE* are shown in the supplementary Table S6, which allowed derivation of the metal occupancies, and some f' and f'' values. The refined Ga occupancies of each metal atom site obtained with *SHELXL* using datasets 3, 8 and 9 are shown in Table 7 (columns 1, 2 and 3), along with those from *JANA*2006, shown in columns 4–7. The derived values of f' and f'' using *MLPHARE* (columns 1 and 2) and *JANA*2006 (columns 3–6) are shown in bold in Table S7 (supplementary material).

4. Discussion

4.1. Dispersive and anomalous difference Fourier maps

The dispersive difference Fourier maps for Zn clearly show that incorporation by Zn into the framework of ZnULM-5 has taken place at the *M*1 and *M*3 sites (Tables 3, S1, Fig. 3*b*), with a greater proportion of Zn at the *M*1 site (average peak height ratio *M*1:*M*3 = 1.28:1). Similarly, the anomalous difference maps for datasets 1, 2, 3 and 7 show peaks at the *M*1 and *M*3 sites (Tables 5, S3, Fig. 5), corroborating the results obtained from the dispersive difference Fourier maps for Zn, with an average ratio of *M*1:*M*3 = 1.41:1.

The dispersive difference maps using the Ga f' dip dataset 9, and datasets 7, 8, 10 and 11 as reference datasets show peaks at each of the metal atom sites, with the four largest, of almost equal peak heights, at the *M*4, *M*6, *M*7 and *M*8 sites, and these can be assumed to be essentially fully occupied Ga sites (Table 4, S2, Fig. 4). The *M*3 followed by the *M*1 sites have reduced peak heights, arising from the incorporation of Zn at these sites, and from the average ratio of the peak heights with respect to the fully occupied Ga sites, the percentages of Ga at the *M*3 and *M*1 sites are estimated to be 71 and 58%, respectively. Assuming that these sites are fully occupied, *i.e.* with Ga + Zn, then the proportions of Zn at the *M*3 and *M*1 sites are thus 29 and 42%, giving an *M*1:*M*3 ratio of 1.45:1, in reasonable agreement with the estimates from the dispersive and anomalous difference maps calculated with the Zn edge data.

Analysis of the anomalous difference maps calculated with data collected around the Ga *K* edge is complicated by the fact that there is a significant signal from both the Zn and Ga metal atoms. In fact, the f'' values for Zn are only slightly smaller than those of Ga for datasets 8 and 10, and it is expected to be significantly larger for dataset 9. Thus, if the *M*1 and *M*3 metal atom sites are assumed to be fully occupied (with Ga plus Zn), which from the single wavelength refinement of the structure is the expectation, then the peak heights in the anomalous difference maps calculated with datasets 8 and 10 should be similar to the sites which are assumed to be fully occupied by Ga, namely the *M*4, *M*6, *M*7 and *M*8 sites, but in fact, they are considerably reduced in height to $\sim$ 50% of the largest peaks. However, the fact that the *M*1 and *M*3 peak heights become the largest with dataset 9 because the f'' value for Zn becomes larger than that for Ga again indicates the incorporation by Zn at these two sites.

Another consistent observation is that the *M*5 and particularly the *M*2 sites show reduced peak heights in the maps arising from a Ga signal, even though there is no indication of Zn incorporation at these sites from the maps calculated using

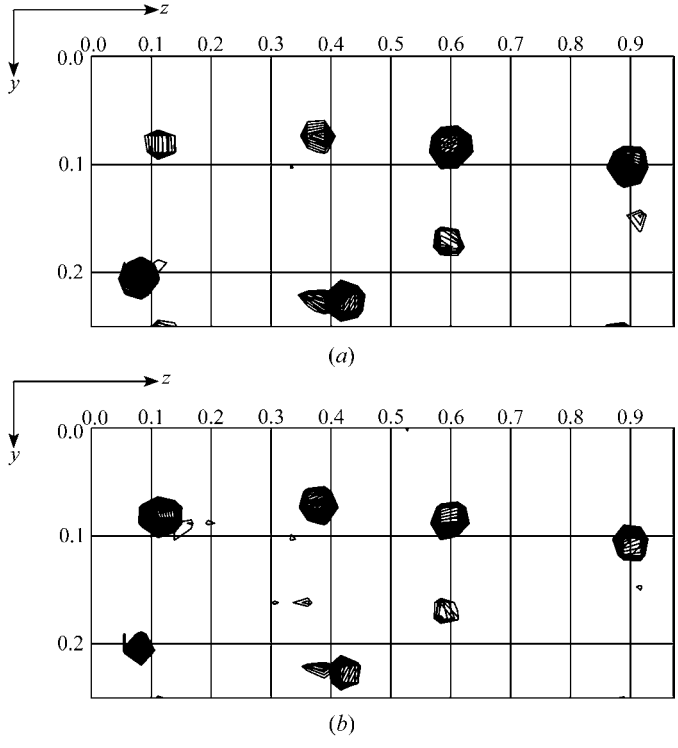

Figure 6
Anomalous difference Fourier map calculated with (*a*) dataset 10, at the f' maximum for Ga, (*b*) dataset 9, where the f'' value for Zn is larger than that of Ga.

Table 7
Refined Ga occupancies derived with *SHELXL* and *JANA*2006.

The first three columns show *SHELXL* refinement against datasets 3, 8 and 9. Columns 4–7 show results from ten-wavelength refinements with *JANA*2006, using values of the dispersive and anomalous coefficients from *MLPHARE*, Model 1, Model 2 and Table 1. NB for Models 1 and 2, *MLPHARE* derived Ga occupancies of 0.78 and 0.82 for sites 1 and 3 were employed (with Zn occupancies of 0.22 and 0.18), and either 1.0 Ga and 0.0 Zn occupancies (Model 1) or 0.95 Ga and 0.05 Zn occupancies (Model 2), for the other metal atom sites.

	SHELXL Dataset 3	*SHELXL* Dataset 8	*SHELXL* Dataset 9	*JANA*2006 (*MLPHARE*)	*JANA*2006 (Model 1)	*JANA*2006 (Model 2)	*JANA*2006 (Table 1)
*M*1	0.77 (1)	0.782 (9)	0.793 (6)	0.795 (2)	0.805 (3)	0.794 (3)	0.781 (2)
*M*3	0.819 (9)	0.806 (9)	0.826 (6)	0.827 (2)	0.843 (3)	0.828 (3)	0.810 (2)
*M*4	0.923 (9)	0.938 (8)	0.947 (5)	0.942 (2)	0.979 (2)	0.950 (2)	0.908 (2)
*M*5	0.918 (9)	0.974 (8)	0.970 (6)	0.948 (2)	0.981 (3)	0.956 (2)	0.920 (2)
*M*6	0.935 (8)	0.926 (8)	0.939 (5)	0.937 (2)	0.969 (2)	0.943 (2)	0.905 (2)
*M*7	0.925 (9)	0.942 (8)	0.955 (5)	0.940 (2)	0.976 (3)	0.948 (2)	0.907 (2)
*M*8	0.937 (9)	0.934 (8)	0.950 (5)	0.934 (2)	0.968 (3)	0.942 (2)	0.905 (2)

datasets giving a signal from Zn alone. The possible reasons are either that these sites have reduced order compared with the other metal atoms sites or that they are partially vacant. In the case of the *M*2 site, it consistently showed higher U_{eq} values in the single wavelength refinements of the structure than the other metal atom sites, including in the Zn-free structure (Loisseu & Ferey, 1994). Using the Zr edge dataset 11 for structure refinement, it was found that this atom could be split into two disordered components, with occupancies constrained to sum to 1.0, thus leading to U_{eq} values much more in keeping with those of the other metal sites. The U_{eq} value for the *M*5 site is also slightly higher than those of the sites which are fully occupied with Ga, but similar to the *M*1 and *M*3 sites, which are disordered because of the mixed Ga/Zn occupancy. Generally, there is some correlation of a U_{eq} refined value with occupancy, *i.e.* although the functional forms of these two parameters are different, in practice, even at a high resolution as we have here, there is probably a correlation. Thus, it seems most likely that the *M*5 site is also fully occupied, but with a slightly higher U_{eq} than average leading to reduced peak heights for this atom.

All the maps have been calculated with data scaled to be approximately on an absolute scale, which should lead to dispersive and anomalous difference Fourier maps which are also on an absolute scale, with peak heights indicating the number of electrons contributing to the signal. Although the peak heights are of the right order with respect to the expected results, for example for the fully occupied Ga atoms from the Ga dispersive difference maps (see Tables 4 and Table S2), the absolute values tend to be somewhat inaccurate, presumably because peak heights are not integrated values of electron density. Thus, although we have been able to identify the sites of incorporation of Zn as the *M*1 and *M*3 sites, it should be possible to obtain more accurate estimations of the occupancies, particularly for the mixed occupancy sites, by refinement, rather than by simply monitoring the peak heights in difference Fourier maps. We discuss this in §4.2. Previously, we showed that *MLPHARE* refinement of the occupancies of the metal atom sites in the Co-substituted chiral microporous zinc phosphate material CoZnPO-CZP allowed improved estimates of the Zn content at each of two metal atom sites to be obtained (Helliwell *et al.*, 1999). In this study, we have used *MLPHARE*, *SHELXL* and *JANA*2006 methods to obtain refined occupancies for the metal atom sites.

4.2. Occupancy refinement of the metal atom sites

4.2.1. Derivation of *f′* and *f″* values and refined metal occupancies using *MLPHARE*. With the multiple wavelength data collections, *MLPHARE* calculations have allowed us to obtain refined absolute values of $\Delta f'$ between various wavelength pairs for each metal atom site, as well as the anomalous signals. The results are shown in Table S6.

In addition, by choosing the $\Delta f'$ values for datasets 8 and 9 with respect to dataset 10, the D10-8 and D10-9 values in Table S6(*a*) give Ga occupancies at the *M*1 and *M*3 sites (the Zn signal is eliminated), which average at 78 and 82%, respectively; the Zn contents are therefore 22 and 18%. These values are only about half those estimated from the peak heights from the difference Fourier maps. However, since the U_{eq} factors from the refinement have been taken into account, and refined, integrated electron values rather than simple peak height estimates have been made with *MLPHARE*, these results should be more reliable than those values obtained from the peak heights. This is also backed up by the fact that the Ga content determined for the *M*2 and *M*5 sites from *MLPHARE* have refined occupancies in keeping with the essentially fully occupied Ga sites, *M*4 and *M*6 to *M*8, thus indicating that these sites are also probably fully occupied by Ga, but have higher atomic displacement parameters than the average.

Another feature of the *MLPHARE* results is that the refined values of $\Delta f'$ and f'' in electrons, on an absolute scale, are close to the expected values for the large Ga signal Table S6(*a*). Thus, it is possible to plot values of f' and f'' for the fully occupied Ga sites, for example *M*4 (Fig. 7*a*). Estimates of the Ga f' value for dataset 8, calculated with different reference datasets vary between *ca* −8.5 and −8.9 electrons, whilst the value of f'' varies between about 1.5 and 2 electrons (Table S7). Similarly, the values of the Ga f' for dataset 9 varies between *ca* −9.0 and −9.4 electrons, and f'' ranges from 0.9 to 1.1 electrons (Table S7). The measured values of f' are in reasonable agreement with the expected values taken from Sasaki (1989), although the reduction in f' for dataset 8 is not

as large as expected for that change in wavelength (Table 1). Similarly, the Ga f'' values for wavelengths 8 and 9 were expected to be 3.9 and ~ 2 electrons, respectively, *i.e.* about twice the values obtained from *MLPHARE*. However, the refined values of f'' for dataset 10 of 3.6 to 4.4 electrons are in good agreement with the Sasaki value of 3.8 electrons. This suggests that the absorption-edge parameters for Ga^{3+} in ZnULM-5 are slightly different to those from Sasaki (1989), which are values calculated for Ga metal.

It is also possible to obtain approximate values at each wavelength, of f' and f'' for Zn at the *M*1 site by subtracting out the signal for Ga and these values, using reference datasets 7 and 11, are plotted *versus* the wavelength in Fig. 7(*b*). By scaling up the values assuming that the Zn occupancy at the *M*1 and *M*3 sites are 0.22 and 0.18, it is also possible to derive values of f' and f'' for Zn for wavelength 3. Using D4-3 (Table S6*b*), where the Ga f' signal should be completely subtracted out, the estimated Zn f' value is -7.2 to -7.4 electrons. From the anomalous occupancies determined with dataset 3, the ANO3 results (Table S6*b*), the derived Zn f'' value at wavelength 3 is 2.4–2.6 electrons. Although these values are approximate owing to the low proportion of Zn compared with Ga at these sites, it suggests that wavelength 3 was not quite at the f' dip for Zn for ZnULM-5, perhaps because of slight wavelength setting inaccuracies, or because the f' dip position from ZnO was not exactly the same as that for Zn in ZnULM-5. However, the wavelength positioning was certainly sufficient to obtain conclusive information regarding the sites of Zn incorporation even though the Zn proportion is low compared with that of Ga.

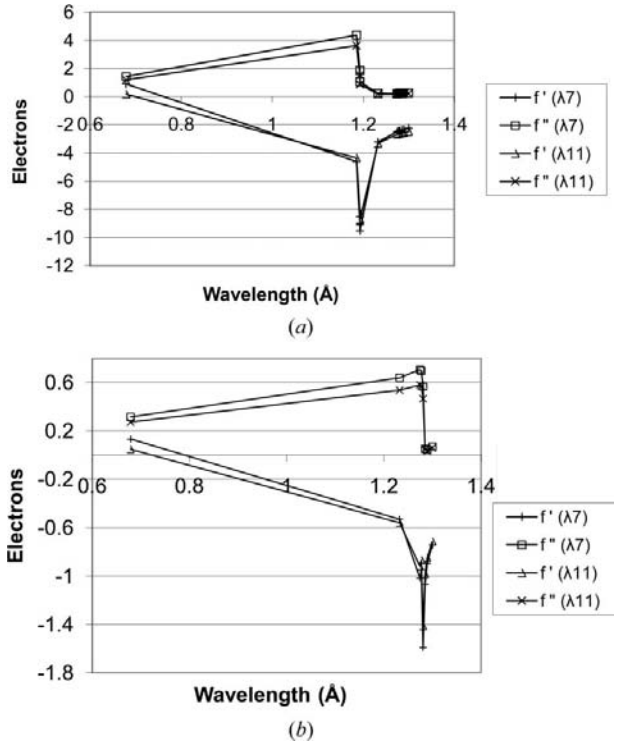

Figure 7
Plots of f' and f'' *versus* wavelength, with values derived from *MLPHARE*, using reference datasets 7 and 11, for the atoms (*a*) *M*4, which is essentially fully occupied by Ga and therefore shows the variation of f' and f'' values for Ga (*b*) *M*1, with the Ga signal subtracted out to show the variation of f' and f'' values for Zn at this site.

4.2.2. Refinement of the metal occupancies using *SHELXL*. Refinement of the occupancies with *SHELXL*, following the method of Cowley *et al.* (2002), gave Ga occupancies for sites *M*1 and *M*3 within experimental error the same as those obtained from *MLPHARE* (Table 7). In addition, refined occupancies for the other metal atom sites indicate that there may be a small incorporation by Zn of between 3 and 8%. It is not possible to determine such a low incorporation of Zn in a site that is predominantly Ga either by difference Fourier techniques, or it seems, by the use of *MLPHARE*. However, the occupancy values from *SHELXL* refinement are sensitive to the input values of f' and f'', and particularly the former. For instance, if the value of the Ga f' is reduced by only 0.5 electron for the refinement of the occupancies against dataset 9, the refinement becomes unstable, whilst an increase of 0.5 electron for the Ga f' value leads to a reduction of refined Ga occupancies for each site by at least 5%. The occupancy values obtained from refinement against the Zn f' dip data are much less sensitive to the input value for f' for Zn, with differences of ± 1 electron only changing the refined occupancies for sites 1 and 3 by up to $\sim 4\%$, but with very little effect on the other predominantly Ga sites, *M*4 through *M*8. The fact that the refined occupancies for each site with datasets 3, 8 and 9 agree closely suggests that the derived values for f' and f'' from *MLPHARE* are reasonably accurate.

4.2.3. Derivation of *f′* and *f″* values and refined metal occupancies using *JANA*2006. In addition to the calculation of f' and f'' values for Zn and Ga with *MLPHARE*, it was also possible to obtain refined values with *JANA*2006, Table S7. These values were then used to carry out refinements of the occupancies of the eight metal atom sites against up to ten wavelengths, using *JANA*2006. The refined values of f' and f'' are in good agreement with those values derived from *MLPHARE*, especially using Model 2. In particular, the Zn f' and f'' values for wavelength 3 are -7.3 and 2.5 electrons from *MLPHARE* and -6.2 (2) and 2.2 (2), and -7.1 (2) and 2.1 (2) electrons from *JANA*2006, Models 1 and 2, respectively. For wavelength 8, the *MLPHARE* values of Ga f' and f'' are -8.7 and 1.75 electrons, whilst for Models 1 and 2 in *JANA*2006, they are -8.42 (2) and 2.53 (2), and -8.69 (2) and 2.49 (2) electrons, respectively; for wavelength 9, the *MLPHARE* values are -9.2 and 1.0 electrons, and for Models 1 and 2, they are -8.86 (2) and 1.23 (2), and -9.14 (2) and 1.22 (2) electrons, respectively. These agreements show there is a small dependence of the output results on the input, *i.e.* starting metal occupancy values. This spread is somewhat larger than the *JANA*2006 standard uncertainty estimates.

Multi-wavelength refinement of the occupancies against up to ten wavelengths was carried out with *JANA*2006, using f' and f'' values derived from *MLPHARE*, and Models 1 and 2, and also the estimated values from Table 1; the refined occupancies are shown in Table 7 (along with those derived using the single wavelength refinement of the occupancies

using *SHELXL*). On the whole, the values agree remarkably closely with one another, particularly those derived using *MLPHARE* and Model 2 values of the dispersive and anomalous coefficients. The values obtained using Model 1 and especially Table 1 values for the coefficients are significantly different, but even the latter occupancies are within a few percent of those from the other models. Tests were also made to investigate the effect of reducing the number of wavelengths used in the refinements, and it was found that for the *MLPHARE*, Model 1 and Model 2 values of f' and f'', the refined occupancies were consistent with those derived using 10 wavelength refinements. For instance, using only wavelengths 3 and 9, and Model 2 values of f' and f'', the Ga occupancies of sites 1 and 3 refined to 0.789 (4) and 0.827 (4), compared with 0.794 (3) and 0.828 (3) from the ten wavelengths refinement. With only one wavelength, either at the f' dip of Zn or that of Ga it was possible to refine the metal occupancies only, keeping the other parameters of the structure fixed. For Model 2 values of f' and f'', the refined occupancies were still within experimental error the same as those derived using the ten wavelength refinement, but with larger standard uncertainties. For wavelength 3, the Ga occupancies of sites 1 and 3 refined to values of 0.782 (7) and 0.824 (7), and for wavelength 9 they were 0.797 (4) and 0.833 (4). The fact that the refined occupancies are so consistent even when reduced numbers of wavelengths are used suggests that the experimentally derived values of f' and f'' for each wavelength are accurate, even at the f' dips of Zn and Ga, where their variation is greatest with small changes in wavelength. It also indicates stability of the wavelength during data collection of each dataset. Conversely, if only wavelengths 3 or 9 were used to refine the metal occupancies using the Table 1 estimates of f' and f'', the refined values altered greatly from the values derived using ten wavelengths; for instance, the Ga occupancies for metal atom sites 1 and 3 derived against wavelength 3 only, refined to values of 0.878 (4) and 0.902 (4), and against wavelength 9 only, values of 0.695 (5) and 0.723 (4) were obtained. Thus we can conclude that fewer than ten wavelengths could be used to derive reasonable metal occupancies by refinement with *JANA*2006, provided that accurate f' and f'' values for each wavelength are known. However, the use of a multi-wavelength approach, using wavelengths both on and more remote from the absorption edges of each metal, safeguards against the effect of possible inaccuracies in the values of f' and f'' on the refined metal occupancies, particularly for wavelengths very close to or on the absorption edges. In addition, the multi-wavelength approach allows the determination of metal atom occupancies to a greater degree of precision than refinement against reduced numbers of wavelengths.

4.3. Structural rationale for the zinc substitution behaviour

The precise chemical reason for the preferential substitution pattern at the *M*1 and *M*3 sites is not known, although a possible explanation is that only the *M*1 and *M*3 sites lie in the cube-like double four-ring (D4R) secondary building unit, which is one of the basic building units in porous framework structures (Baerlocher *et al.*, 2001). The D4R building units in the ULM-5 structure consist of *M*1 and *M*3 metal atoms arranged alternately with tetrahedrally bound P atoms into the cube-like D4R structure, with an encapsulated F atom within each cube (Loiseau & Ferey, 1994). Specifically, it is found that in metal-substituted microporous aluminophosphates and aluminosilicates which contain D4R building units, hetero atoms tend to incorporate preferentially and to a greater degree, into sites within these building units. This is explained by the possibility of relaxation or distortion of the D4R framework which allows the isomorphous substitution of hetero atoms (Mellot-Draznieks *et al.*, 2002). The preferential incorporation of hetero atoms into framework sites with higher coordination numbers that was reported for many metal-substituted zeotype structures, as well as the charge compensating factor, where the presence of extra framework cations or fluoride anions influence the extent and position of metal incorporation (Pastore *et al.*, 2005), do not seem to play a crucial role in the formation of the ZnULM-5 structure.

The Zn concentration determined by the crystallographic analysis is lower than that found by the EDAX analysis of five different crystals, *i.e.* 3–6 wt % (Mrak *et al.*, 2001). This is even when, in addition to the substitution at the *M*1 and *M*3 sites of ~ 22 and 18%, the possible Zn incorporation to an extent of about 5% over the other metal atom sites is considered. This is most probably due to the inhomogenity of the Zn distribution over the crystals or from the surface towards the subsurface region of the crystals, which is quite common in metal-substituted zeotype materials.

4.4. Methodology implications

The results presented here show that the multi-wavelength approach has been extremely effective in allowing the selection of signals from each of these neighbouring elements in turn. The difference Fourier maps have allowed the sites of Zn incorporation to be identified, and more precise estimates of dispersive and anomalous differences have been possible by refinement of dispersive and anomalous occupancies using the program *MLPHARE* and by refinement of the occupancies of the metal atom sites with *SHELXL* and most reliably, with multi-wavelength refinement using *JANA*2006. Moreover, in addition to the determination of metal incorporation in ZnULM-5 by dispersive difference methods, it has also been possible to obtain further information using anomalous difference techniques for this non-centrosymmetric sample, which reinforce the results obtained using differences in f'. This is in contrast to the previously investigated non-centrosymmetric compound CoZnPO-CZP which gave clear-cut results from dispersive difference Fourier maps, but inconclusive results from the anomalous difference maps, particularly regarding the incorporated Co, which was present at a level of only 20% of the total metal atom content. The calculated values of the average anomalous dispersion, AD (Helliwell *et al.*, 2005), for Co and Zn in CoZnPO-CZP at the Co f'' maximum were 2.6 and 3.5%, respectively, thus being

rather small and similar in value, but the calculated AD for Zn of 14.0% at the Zn f'' maximum was expected to give rise to a signal, but the result was not clear cut. In that case, it was assumed that the lack of a signal arose because of the low resolution of the datasets, which meant that there were very few Friedel pairs of reflections for the calculation of the anomalous difference maps (19 and 42 reflection pairs at the Co and Zn *K* edges, respectively). With the much improved detector provision at SRS Daresbury Station 9.8, which comprised a CCD APEXII detector and D8 diffractometer with a 2θ tilt arm, it was possible to obtain data to at least 0.85 Å and high completeness at all 11 measured wavelengths. Thus, although the AD for Zn for wavelength 1, for example, was only 2.0%, because the data were measured to high resolution, there were 3440 Friedel pairs, and therefore the incorporation at the *M*1 and *M*3 sites could be determined from an anomalous difference Fourier map and by refinement of the anomalous occupancies. For datasets 8 and 10, the AD for Ga is $\sim$ 13.8%, whereas that for Zn is only 1.7%, so that the Zn signal is effectively swamped by that of Ga. However, the situation is more favourable for dataset 9, where the AD for Zn is 1.8% but that for Ga is reduced to 3.7% (estimated using the experimentally determined value of f'' for Ga of 1 electron) and we therefore obtained enhancement of the two sites which contain Zn.

5. Conclusions

This experiment was a challenging one and as a measure of that, the number of wavelengths used here must be a record. The wavelength setting on SRS 9.8 was not rapidly tunable in contrast to beamlines with a double crystal monochromator but, although relatively laborious, led to wavelength settings that were true to expectation, and data collection of 11 datasets at different wavelengths, within a period of 3 d of beam time. The use of the full 2θ swing arm type of diffractometer allowed the diffraction resolution to be at least 0.85 Å, thus allowing standard model refinement, and a great improvement on our earlier work with CoZnPO-CZP (Helliwell *et al.*, 1999). The use of dispersive and anomalous difference Fourier electron-density maps gave both a useful immediate picture of the substitution patterns and *via* peak-height comparisons, a semi-quantitative indication of occupancies of Zn and Ga at the eight sites. The fully quantitative determinations of the dispersive and anomalous coefficients for Ga and Zn at each wavelength, as well as metal atom occupancies over the eight metal atom sites were made from use of the CCP4's *MLPHARE* program as well as *SHELXL* and *JANA*2006. The results by these methods agree closely (Table 7), and *JANA*2006 allowed the ready determination of standard uncertainties on the occupancy parameters. In addition, *SCALEIT* from CCP4 gave r.m.s. differences within and across dataset pairs for dataset dispersive and anomalous diffraction signals' evaluation. Also, the *MLPHARE* calculation involving probability estimates of reflection phases from Harker phasing diagrams, yields 'best phase' estimates (Blow & Crick, 1959). These 'best phases' showed that the whole of the structure of the framework was defined from the MAD signals from the Ga and Zn.

Structurally, the location of isomorphously substituted zinc over the crystallographically different gallium sites has been determined to occur predominantly at two sites of the eight, to an extent of $\sim$ 22 and 18% at the *M*1 and *M*3 sites, respectively. The preferential substitution of Zn at these sites probably arises because they are located in D4R building units which can relax to accommodate the incorporation of hetero atoms.

For the future, the relative ease with which multiple wavelength datasets can now be measured and analysed points to site-specific information being much more readily obtainable as a function of a variety of functional and chemical changes such as due to oxidation/reduction, pH change and temperature.

We thank Daresbury Laboratory for provision of beam time on the SRS. We thank The Royal Society for a research collaboration agreement between Manchester and Ljubljana thus facilitating reciprocal visits between the two research centres. We thank the School of Chemistry, University of Manchester and the National Institute of Chemistry, Ljubljana, for general support.

References

Arndt, U. W., Greenhough, T. J., Helliwell, J. R., Howard, J. A. K., Rule, S. A. & Thompson, A. W. (1982). *Nature*, **298**, 835–838.
Baerlocher, Ch., Olson, D. H. & Meier, W. M. (2001). *Atlas of Zeolite Framework Types.* Amsterdam: Elsevier.
Blow, D. M. & Crick, F. H. C. (1959). *Acta Cryst.* **12**, 794–802.
Bruker (2001*a*). *SMART*, Version 5.625. Bruker AXS Inc., Madison, Wisconsin, USA.
Bruker (2001*b*). *SADABS*, Version 2.03*a.* Bruker AXS Inc., Madison, Wisconsin, USA.
Bruker (2001*c*). *SHELXTL*, Version 6.12. Bruker AXS Inc., Madison, Wisconsin, USA.
Bruker (2002). *SAINT*, Version 6.36*a.* Bruker AXS Inc., Madison, Wisconsin, USA.
Cernik, R. J., Clegg, W., Catlow, C. R. A., Bushnell-Wye, G., Flaherty, J. V., Greaves, G. N., Burrows, I., Taylor, D. J., Teat, S. J. & Hamichi, M. (1997). *J. Synchrotron Rad.* **4**, 279–286.
Cheetham, A. & Wilkinson, A. P. (1992). *Angew. Chem. Int. Ed. Engl.* **31**, 1557–1570.
Cianci, M., Helliwell, J. R., Helliwell, M., Kaucic, V., Logar, N. Z., Mali, G. & Tusar, N. N. (2005). *Crystallogr. Rev.* **11**, 245–335.
Collaborative Computational Project, Number 4 (1994). *Acta Cryst.* D**50**, 760–763.
Cowley, A. R., Jones, R. H., Teat, S. J. & Chippindale, A. M. (2002). *Microporous Mesoporous Mater.* **51**, 51–64.
Cromer, D. T. (1983). *J. Appl. Cryst.* **16**, 437.
Flack, H. D. & Bernardinelli, G. (1999). *Acta Cryst.* A**55**, 908–915.
Hartmann, M. & Kevan, L. (1999). *Chem. Rev.* **99**, 635–663.
Helliwell, J. R. (1984). *Rep. Prog. Phys.* **47**, 1403–1497.
Helliwell, J. R., Greenhough, T. J., Carr, P., Rule, S. A., Moore, P. R., Thompson, A. W. & Worgan, J. S. (1982). *J. Phys. E*, **15**, 1363–1372.
Helliwell, M., Helliwell, J. R., Kaucic, V., Zabukovec Logar, N., Barba, L., Busetto, E. & Lausi, A. (1999). *Acta Cryst.* B**55**, 327–332.
Helliwell, M., Jones, R. H., Kaucic, V. & Logar, N. Z. (2005). *J. Synchrotron Rad.* **12**, 420–430.
Hodeau, J. L., Favre-Nicoli, V., Bos, S., Renevier, H., Lorenzo, E. & Berar, J.-F. (2001). *Chem. Rev.* **101**, 1843–1867.

Loiseau, T. & Ferey, G. (1994). *J. Solid State Chem.* **111**, 403–415.
Mellot-Draznieks, C., Girard, S. & Ferey, G. (2002). *J. Am. Chem. Soc.* **124**, 15326–15335.
Mrak, M., Helliwell, M., Ristic, A., Zabukovec Logar, N. & Kaucic, V. (2001). *Acta Chim. Slov.* **48**, 147–158.
Otwinowski, Z. & Minor, W. (1997). *Methods in Enzymology*, Vol. 276, *Macromolecular Crystallography*, part A, edited by C. W. Carter Jr & R. M. Sweet, pp. 307–326. New York: Academic Press.
Pastore, H. O., Coluccia, S. & Marchese, L. (2005). *Annu. Rev. Mater. Res.* **35**, 351–365.
Petricek, V., Dusek, M. & Palatinus, L. (2006). *JANA*2006. Institute of Physics, Praha, Czech Republic.
Sasaki, S. (1989). *KEK*, Report 88–14. National Laboratory for High Energy Physics, Tsukuba, Japan.
Sheldrick, G. M. (2008). *Acta Cryst.* A**64**, 112–122.
Wu, G., Zhang, Y., Ribaud, L., Coppens, P., Wilson, C., Iversen, B. B. & Larsen, F. K. (1998). *Inorg. Chem.* **37**, 6078–6083.
Zhang, Y., Wilkinson, A. P., Lee, P. L., Shastri, S. D., Shu, D., Chung, D.-Y. & Kanatzidis, M. G. (2005). *J. Appl. Cryst.* **38**, 433–441.
Zhang, Y., Wilkinson, A. P., Nolas, G. S., Lee, P. L. & Hodges, J. P. (2003). *J. Appl. Cryst.* **36**, 1182–1189.